






Outside-Obstacle Representations with All Vertices on the Outer Face

Oksana Firman¹, Philipp Kindermann², Jonathan Klawitter¹,
Boris Klemz¹, Felix Klesen¹, and Alexander Wolff¹

¹ Institut für Informatik, Universität Würzburg, Germany
`firstname.lastname@uni-wuerzburg.de`

² Informatikwissenschaften, Universität Trier, Germany
`kindermann@uni-trier.de`

Abstract. An *obstacle representation* of a graph G consists of a set of polygonal obstacles and a drawing of G as a *visibility graph* with respect to the obstacles: vertices are mapped to points and edges to straight-line segments such that each edge avoids all obstacles whereas each non-edge intersects at least one obstacle. Obstacle representations have been investigated quite intensely over the last few years. Here we focus on *outside-obstacle representations* (OORs) that use only one obstacle in the outer face of the drawing. It is known that every outerplanar graph admits such a representation [Alpert, Koch, Laison; DCG 2010].

We strengthen this result by showing that every (partial) 2-tree has an OOR. We also consider restricted versions of OORs where the vertices of the graph lie on a convex polygon or a regular polygon. We characterize when the complement of a tree and when a complete graph minus a simple cycle admits a convex OOR. We construct regular OORs for all (partial) outerpaths, cactus graphs, and grids.

Keywords: obstacle representation · visibility graph · outside obstacle

1 Introduction

Recognizing graphs that have a certain type of geometric representation is a well-established field of research dealing with, e.g., geometric intersection graphs, visibility graphs, and graphs admitting certain contact representations. Given a set \mathcal{C} of *obstacles* (here, simple polygons without holes) and a set P of points in the plane, the *visibility graph* $G_{\mathcal{C}}(P)$ has a vertex for each point in P and an edge pq for any two points p and q in P that can *see* each other, that is, the line segment \overline{pq} connecting p and q does not intersect any obstacle in \mathcal{C} . An *obstacle representation* of a graph G consists of a set \mathcal{C} of obstacles in the plane and a mapping of the vertices of G to a set P of points such that $G = G_{\mathcal{C}}(P)$. The mapping defines a straight-line drawing Γ of $G_{\mathcal{C}}(P)$. We planarize Γ by replacing all intersection points by dummy vertices. The outer face of the resulting planar drawing is a closed polygonal chain Π_{Γ} where vertices and edges can occur several times. We call the complement of the closure of Π_{Γ} the *outer face* of Γ .

We differentiate between two types of obstacles: *outside* obstacles lie in the outer face of the drawing, and *inside* obstacles lie in the complement of the outer face; see Fig. 1a.

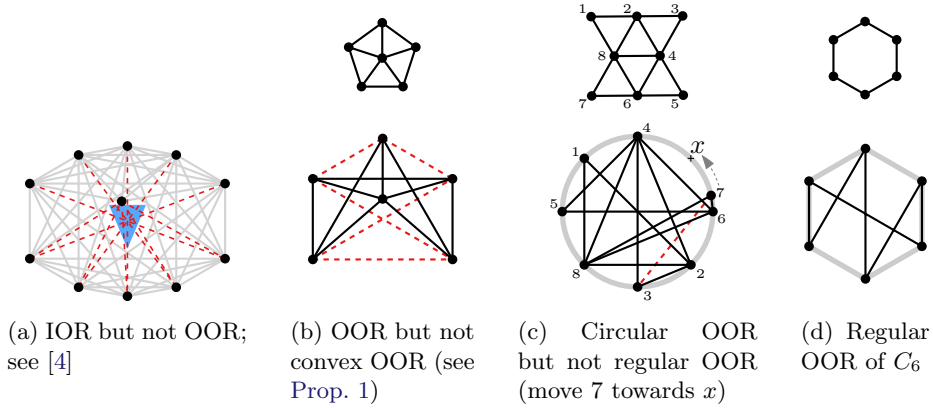


Fig. 1: Inside- and outside-obstacle representations (IORs and OORs).

Every graph trivially admits an obstacle representation: take an arbitrary straight-line drawing without collinear vertices and “fill” each face with an obstacle. This, however, can lead to a large number of obstacles, which motivates the optimization problem of finding an obstacle representation with the minimum number of obstacles. For a graph G , the *obstacle number* $\text{obs}(G)$ is the smallest number of obstacles that suffice to represent G as a visibility graph.

In this paper, we focus on *outside* obstacle representations (OORs), that is, obstacle representations with a single outside obstacle and without any inside obstacles. For such a representation, it suffices to specify the positions of the vertices; the outside obstacle is simply the whole outer face of the representation. In an OOR every non-edge must thus intersect the outer face. We also consider three special types: In a *convex* OOR, the vertices must be in convex position; in a *circular* OOR, the vertices must lie on a circle; and in a *regular* OOR, the vertices must form a regular n -gon.

In general, the class of graphs representable by outside obstacles is not closed under taking subgraphs, but the situation is different for graphs admitting a *reducible* OOR, meaning that all of its edges are incident to the outer face:

Observation 1. *If a graph G admits a reducible OOR, then every subgraph of G also admits such a representation.*

Previous Work. Alpert et al. [1] introduced the notion of the obstacle number of a graph in 2010. They also introduced *inside* obstacle representations, i.e., representations without an outside obstacle. They characterized the class of graphs that have an inside obstacle representation with a single convex obstacle and

showed that every outerplanar graph has an OOR. Chaplick et al. [4] proved that the class of graphs with an inside obstacle representation is incomparable with the class of graphs with an OOR. They showed that any graph with at most seven vertices has an OOR, which does not hold for a specific 8-vertex graph.

Alpert et al. [1] further showed that $\text{obs}(K_{m,n}^*) \leq 2$ for any $m \leq n$, where $K_{m,n}^*$ is the complete bipartite graph $K_{m,n}$ minus a matching of size m . They also proved that $\text{obs}(K_{5,7}^*) = 2$. Pach and Sariöz [10] showed that $\text{obs}(K_{5,5}^*) = 2$. Berman et al. [3] suggested some necessary conditions for a graph to have obstacle number 1. They gave a SAT formula that they used to find a *planar* 10-vertex graph (with treewidth 4) that has no 1-obstacle representation.

Obviously, any n -vertex graph has obstacle number $\mathcal{O}(n^2)$. Balko et al. [2] improved this to $\mathcal{O}(n \log n)$. Dujmović and Morin [5] showed that there are n -vertex graphs whose obstacle number is $\Omega(n/(\log \log n)^2)$, improving previous lower bounds [1,9,8]. They also pointed out that grid graphs admit OORs.

Our Contribution. We first strengthen the result of Alpert et al. [1] regarding OORs of outerplanar graphs by showing that every (partial) 2-tree admits a reducible OOR with all vertices on the outer face; see Section 2. Equivalently, every graph of treewidth at most two, which includes outerplanar and series-parallel graphs, admits such a representation. Then we establish two combinatorial conditions for convex OORs (see Section 3). In particular, we introduce a necessary condition that can be used to show that a given graph does *not* admit a convex OOR as, e.g., the graph in Fig. 1b. We apply these conditions to characterize when the complement of a tree and when a complete graph minus a simple cycle admits a convex OOR. We construct *regular* reducible OORs for all outerpaths, grids, and cacti; see Section 4. The result for grids strengthens the aforementioned observation by Dujmović and Morin [5].

We postpone the proofs of statements with a (clickable) “★” to the appendix.

Notation. For a graph G , let $V(G)$ be the vertex set of G , and let $E(G)$ be the edge set of G . Arranging the vertices of G in circular order $\sigma = \langle v_1, \dots, v_n \rangle$, we write, for $i \neq j$, $[v_i, v_j]$ to refer to the sequence $\langle v_i, v_{i+1}, \dots, v_{j-1} \rangle$, where indices are interpreted modulo n . Sequences (v_i, v_j) and $[v_i, v_j]$ are defined analogously.

2 Outside-Obstacle Representations for Partial 2-Trees

The graph class of *2-trees* is recursively defined as follows: K_3 is a 2-tree. Further, any graph is a 2-tree if it is obtained from a 2-tree G by introducing a new vertex x and making x adjacent to the endpoints of some edge uv in G . We say that x is *stacked* on uv . The edges xu and xv are called the *parent edges* of x .

Theorem 1 (★). *Every 2-tree admits a reducible OOR with all vertices on the outer face.*

Proof sketch. Every 2-tree T can be constructed through the following iterative procedure: (1) Start with one edge, called the *base* edge and mark its vertices

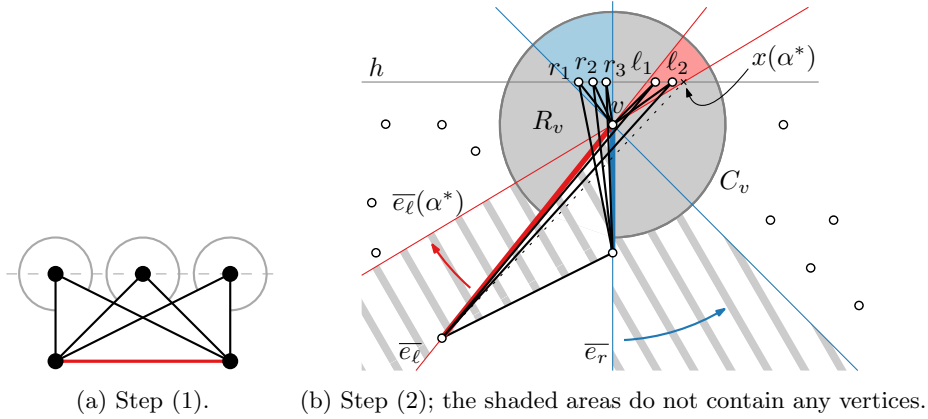


Fig. 2: Construction steps in the proof of [Theorem 1](#).

as *inactive*. Stack any number of vertices onto the base edge and mark them as *active*. During the entire procedure, every present vertex is marked either as active or inactive. Moreover, once a vertex is inactive, it remains inactive for the remainder of the construction. (2) Pick one active vertex v and stack any number of vertices onto each of its two parent edges. All the new vertices are marked as active and v as inactive. (3) If there are active vertices remaining, repeat step (2). We construct a drawing of T by geometrically implementing this iterative procedure, so that after every step of the algorithm the present part of the graph is realized as a straight-line drawing satisfying the following invariants:

- (i) Each vertex v not incident to the base edge is associated with an open circular arc C_v that lies completely in the outer face and whose endpoints belong to the two parent edges of v . Moreover, v is located at the center of C_v and the parent edges of v are below v .
- (ii) Each non-edge intersects the circular arc of at least one of its incident vertices.
- (iii) For each active vertex v , the region R_v enclosed by C_v and the two parent edges of v is *empty*, meaning that R_v is not intersected by any edges, vertices, or circular arcs.
- (iv) Every vertex is incident to the outer face.

It is easy to see that once the procedure terminates with a drawing that satisfies invariants (i)–(iv), we obtain the desired representation (in particular, invariants (i) and (ii) together imply that each non-edge intersects the outer face).

Construction. To carry out step (1), we draw the base edge horizontally and place the stacked vertices on a common horizontal line above the base edge, see [Fig. 2a](#). Circular arcs that satisfy the invariants are now easy to define. Suppose we have obtained a drawing Γ of the graph obtained after step (1) and some number of iterations of step (2) such that Γ is equipped with a set

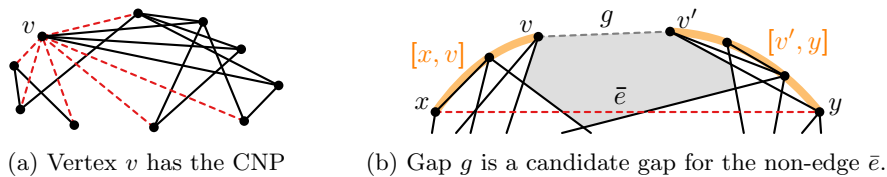


Fig. 3: Examples for the consecutive-neighbors property (CNP) and a candidate gap.

of circular arcs satisfying the invariants (i)–(iv). We describe how to carry out another iteration of step (2) while maintaining the invariants. Let v be an active vertex. By invariant (i), both parent edges of v are below v . Let e_ℓ and e_r be the left and right parent edge, respectively. Let $\ell_1, \ell_2, \dots, \ell_i$ and r_1, r_2, \dots, r_j be the vertices stacked onto e_ℓ and e_r , respectively. We refer to $\ell_1, \ell_2, \dots, \ell_i$ and r_1, r_2, \dots, r_j as the *new* vertices; the vertices of Γ are called *old*. We place all the new vertices on a common horizontal line h that intersects R_v above v , see Fig. 2b. The vertices $\ell_1, \ell_2, \dots, \ell_i$ are placed inside R_v , to the right of the line \bar{e}_ℓ extending e_ℓ . Symmetrically, r_1, r_2, \dots, r_j are placed inside R_v , to the left of the line \bar{e}_r extending e_r .

We place $\ell_1, \ell_2, \dots, \ell_i$ close enough to e_ℓ and r_1, r_2, \dots, r_j close enough to e_r such that the following properties are satisfied: (a) None of the parent edges of the new vertices intersect C_v . (b) For each new vertex, the unbounded open cone obtained by extending its parent edges to the bottom does not contain any vertices.

Each of the old vertices retains its circular arc from Γ . By invariants (i) and (iii) for Γ , it is easy to define circular arcs for the new vertices that satisfy invariant (i). Using invariants (i)–(iv) for Γ and properties (a) and (b), it can be shown that all invariants are satisfied. \square

3 Convex Outside Obstacle Representations

We start with a sufficient condition. Suppose that we have a convex OOR Γ of a graph G . Let σ be the clockwise circular order of the vertices of G along the convex hull. If all neighbors of a vertex v of G are consecutive in σ , we say that v has the *consecutive-neighbors property*, which implies that all non-edges incident to v are consecutive around v and trivially intersect the outer face in the immediate vicinity of v ; see Fig. 3a.

Lemma 1 (Consecutive-neighbors property). *A graph G admits a convex OOR with circular vertex order σ if there is a subset V' of $V(G)$ that covers all non-edges of G and each vertex of V' has the consecutive-neighbors property with respect to σ .*

Next, we derive a necessary condition. For any two consecutive vertices v and v' in σ that are not adjacent in G , we say that the line segment $g = \overline{vv'}$ is a *gap*. Then the *gap region* of g is the inner face of $\Gamma + vv'$ incident to g ; see the gray region in Fig. 3b. We consider the gap region to be open, but add to it

the relative interior of the line segment $\overline{vv'}$, so that the non-edge vv' intersects its own gap region. Observe that each non-edge $\bar{e} = xy$ that intersects the outer face has to intersect some gap region in an OOR. Suppose that g lies between x and y with respect to σ , that is, $[v, v'] \subseteq [x, y]$. We say that g is a *candidate gap* for \bar{e} if there is no edge that connects a vertex in $[x, v]$ and a vertex in $[v', y]$. Note that \bar{e} can only intersect gap regions of candidate gaps.

Lemma 2 (Gap condition). *A graph G admits a convex OOR with circular vertex order σ only if there exists a candidate gap with respect to σ for each non-edge of G .*

It remains an open problem whether the gap condition is also sufficient. Nonetheless, we can use the gap condition for no-certificates. To this end, we derived a SAT formula from the following expression, which checks the gap condition for every non-edge of a graph G :

$$\bigwedge_{xy \notin E(G)} \left[\bigvee_{v \in [x, y]} \left(\bigwedge_{u \in [x, v], w \in (v, y]} uv \notin E(G) \right) \vee \bigvee_{v \in [y, x]} \left(\bigwedge_{u \in [y, v], w \in (v, x]} uv \notin E(G) \right) \right]$$

We have used this formula to test whether all connected cubic graphs with up to 16 vertices admit convex OORs. The only counterexample we found was the Petersen graph. The so-called Blanusa snarks, the Pappus graph, the dodecahedron, and the generalized Peterson graph $G(11, 2)$ satisfy the gap condition. The latter three graphs do admit convex OORs [6].

The smallest graph (and the only 6-vertex graph) that does not satisfy the gap condition is the wheel graph W_6 (see Prop. 1 in Appendix A). Hence, W_6 does not admit a *convex* OOR, but it does admit a (non-convex) OOR; see Fig. 1b.

In the following, we consider “dense” graphs, namely the complements of trees. For any graph G , let $\bar{G} = (V(G), \bar{E}(G))$ with $\bar{E}(G) = \{uv \mid uv \notin E(G)\}$ be the complement of G . A *caterpillar* is a tree where all vertices are within distance at most 1 of a central path.

Theorem 2 (★). *For any tree T , the graph \bar{T} has a convex OOR if and only if T is a caterpillar.*

Proof sketch. First, we show that for every caterpillar C , the graph \bar{C} has a circular OOR. To this end, we arrange the vertices of the central path P on a circle in the order given by P . Then, for each vertex of P , we insert its leaves as an interval next to it; see Fig. 10 in Appendix B. The result is a circular OOR since every non-edge of \bar{C} intersects the outer face in the vicinity of the incident path vertex (or vertices). Second, we show that if T is a tree that is not a caterpillar, then for any circular vertex order, there exists at least one non-edge of \bar{T} that is a diagonal of a quadrilateral formed by edges of \bar{T} . \square

Another class of dense graphs consists of complete graphs from which we remove the edge set of a simple (not necessarily Hamiltonian) cycle. Using Lemma 2, we can prove the following theorem similarly as Theorem 2.

Theorem 3 (★). *Let $3 \leq k \leq n$. Then the graph $G_{n,k} = K_n - E(C_k)$, where C_k is a simple k -cycle, admits a convex OOR if and only if $k \in \{3, 4, n\}$.*

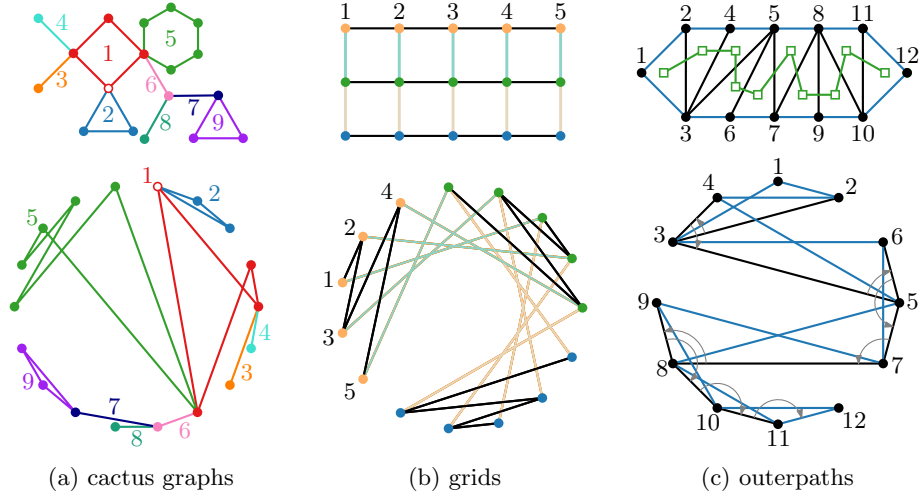


Fig. 4: Graph classes that admit reducible regular OORs (see Theorem 4).

4 Regular Outside Obstacle Representations

This section deals with regular OORs. A *cactus* is a connected graph where every edge is contained in at most one simple cycle. An *outerpath* is a graph that admits an *outerpath* drawing, i.e., an outerplanar drawing whose weak dual is a path. A *grid* is the Cartesian product $P_k \square P_\ell$ of two simple paths P_k, P_ℓ .

Theorem 4 (\star). *The following graphs have reducible regular OORs:*
 1. every cactus; 2. every grid; 3. every outerpath.

Proof sketch. For cacti, we use a decomposition into *blocks* (i.e., maximal 2-connected subgraphs or bridges). We start with an arbitrary block and insert its child blocks as intervals next to the corresponding cut vertices etc.; see Fig. 4a. For a grid, we lay out each horizontal path in a separate arc, in a zig-zag manner. Then we add the vertical edges accordingly; see Fig. 4b. Our strategy for (maximal) outerpaths relies on a specific stacking order. We start with a triangle. Then we always place the next inner edge (black in Fig. 4c) such that it avoids the empty arc that corresponds to the previous inner edge. \square

Every graph with up to six vertices – except for the graph in Fig. 1b – and every outerplanar graph with up to seven vertices admits a regular OOR (see Prop. 1 in Appendix A and [7], respectively). The 8-vertex outerplanar graph in Fig. 1c (and only it [7]), however, does not admit any regular OOR (see Prop. 2).

Our representations for cacti, outerpaths, and complements of caterpillars depend only on the vertex order. Hence, given such a graph with n vertices, every cocircular point set of size n is *universal*, i.e., can be used for an OOR.

5 Open Problems

- (1) What is the complexity of deciding whether a given graph admits an OOR?
- (2) Is the gap condition sufficient, i.e., does every graph with a circular vertex order satisfying the gap condition admit a convex OOR?
- (3) Does every graph that admits a *convex* OOR also admit a *circular* OOR?
- (4) Does every outerplanar graph admit a (reducible) convex OOR?
- (5) Does every connected cubic graph *except the Peterson graph* admit a convex OOR?

References

1. Hannah Alpert, Christina Koch, and Joshua D. Laison. Obstacle numbers of graphs. *Discrete Comput. Geom.*, 44(1):223–244, 2010. doi:10.1007/s00454-009-9233-8.
2. Martin Balko, Josef Cibulka, and Pavel Valtr. Drawing graphs using a small number of obstacles. *Discrete Comput. Geom.*, 59(1):143–164, 2018. doi:10.1007/s00454-017-9919-2.
3. Leah Wrenn Berman, Glenn G. Chappell, Jill R. Faudree, John Gimbel, Chris Hartman, and Gordon I. Williams. Graphs with obstacle number greater than one. *J. Graph Algorithms Appl.*, 21(6):1107–1119, 2017. doi:10.7155/jgaa.00452.
4. Steven Chaplick, Fabian Lipp, Ji-won Park, and Alexander Wolff. Obstructing visibilities with one obstacle. In Yifan Hu and Martin Nöllenburg, editors, *Proc. 24th Int. Symp. Graph Drawing & Network Vis. (GD)*, volume 9801 of *Lect. Notes Comput. Sci.*, pages 295–308. Springer-Verlag, 2016. URL: <http://arxiv.org/abs/1607.00278>, doi:10.1007/978-3-319-50106-2_23.
5. Vida Dujmović and Pat Morin. On obstacle numbers. *Electr. J. Combin.*, 22(3):paper #P3.1, 7 pages, 2015. See also [arxiv.org/1308.4321](http://arxiv.org/abs/1308.4321). doi:10.37236/4373.
6. Christian Goldschmied. 1-Hindernis-Sichtbarkeitsgraphen von kubischen Graphen. Bachelor’s thesis, Institut für Informatik, Universität Würzburg, 2021. URL: <http://www1.pub.informatik.uni-wuerzburg.de/pub/theses/2021-goldschmied-bachelor.pdf>.
7. León Lang. Regelmäßige Außenhindernisrepräsentation von kleinen planaren Graphen. Bachelor’s thesis, Institut für Informatik, Universität Würzburg, 2022. URL: <http://www1.pub.informatik.uni-wuerzburg.de/pub/theses/2022-lang-bachelor.pdf>.
8. Padmini Mukkamala, János Pach, and Dömötör Pálvölgyi. Lower bounds on the obstacle number of graphs. *Electr. J. Combin.*, 19(2):paper #P32, 8 pages, 2012. URL: <http://www.combinatorics.org/ojs/index.php/eljc/article/view/v19i2p32>.
9. Padmini Mukkamala, János Pach, and Deniz Sariöz. Graphs with large obstacle numbers. In Dimitrios M. Thilikos, editor, *Proc. Conf. Graph-Theoretic Concepts Comput. Sci. (WG)*, volume 6410 of *Lect. Notes Comput. Sci.*, pages 292–303. Springer-Verlag, 2010. doi:10.1007/978-3-642-16926-7_27.
10. János Pach and Deniz Sariöz. On the structure of graphs with low obstacle number. *Graphs & Combin.*, 27(3):465–473, 2011. doi:10.1007/s00373-011-1027-0.

Appendix

A Small Graphs

Proposition 1. *There exists a regular OOR for every graph with up to six vertices, except for the wheel graph W_6 .*

Proof. Note that W_6 is isomorphic to $G_{6,5} = K_6 - E(C_5)$. Hence, by [Theorem 3](#), W_6 does not admit a convex OOR.

Except the excluded one, all graphs satisfy the gap condition: For graphs with up to four vertices, this is not difficult to check. For graphs with five vertices, see [Fig. 5](#). For graphs with six vertices consider the following cases occurring when

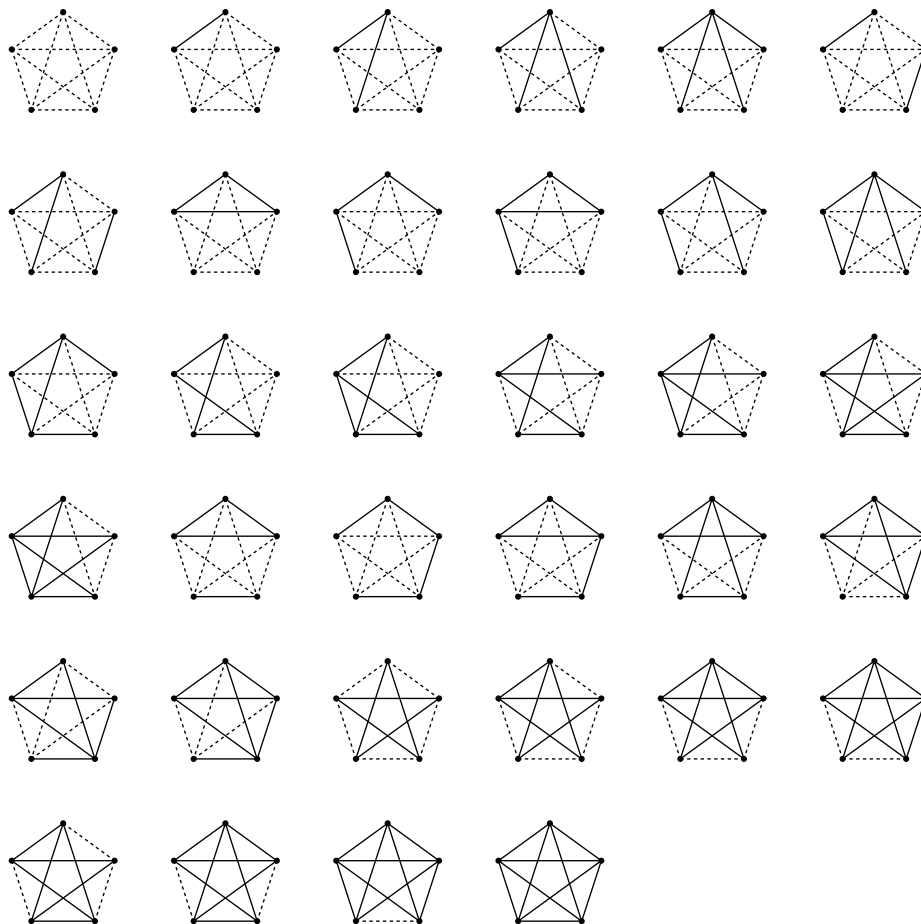


Fig. 5: Every graph with up to five vertices admits a regular OOR.

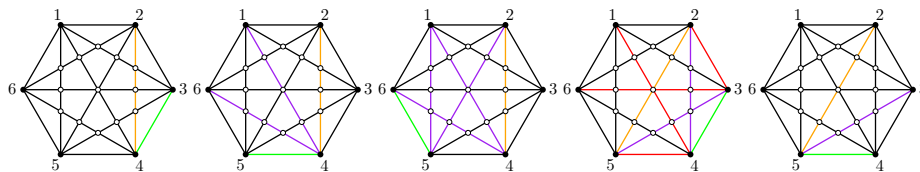


Fig. 6: Given the orange non-edge, there are different green non-edges through which the gap-condition could be satisfied. The purple non-edges are additionally enforced by the gap-conditions satisfaction.

drawing any permutation satisfying the gap condition on the hexagon:

- A non-edge on the outer face is obviously visible.
- For a non-edge of length 2 (for instance between vertices 2 and 4 in Fig. 6), there are three possible gaps, through which it could be visible (depicted with a green non-edge). The gap condition further enforces all non-edges depicted in purple, such that in all three cases the orange non-edge is visible.
- If the orange non-edge spans length 3, there are two possibly used gaps and the first of these does not work geometrically, since the orange non-edge could only be cut at the center point, which, however, would also cut two edges. (Red edges are enforced by the case distinction.)

To solve this case we argue, that for all graphs having this pattern, there is also another permutation without this problem. To this end see Fig. 7. The first row depicts all possible graphs with the problematic pattern and the second row their respective alternative permutation. We group the graphs according to the non-edges on the outer cycle.

- In the first column is the case, where all pairs of vertices not explicitly given from the pattern are edges.
- In the second case 12 and 56 are non-edges. Note that we can hence require the edges 15 and 26, since if either is missing, we do not need to change the drawing. All other possible edges (depicted in gray) are undecided.
- The third case has non-edges 12 and 16, such that we may require the edges 26, 56 and 46.
- The fourth case has non-edge 12.
- The fifth case has non-edge 16.

This gives us a working permutation for every graph with the problematic pattern. \square

Proposition 2. *There exists an 8-vertex outerplanar graph that has no regular OOR.*

Proof. Consider the 6-vertex outerplanar graph G in Fig. 8. Up to rotation and mirroring, it has only two regular OORs, which we tested using a variant of the

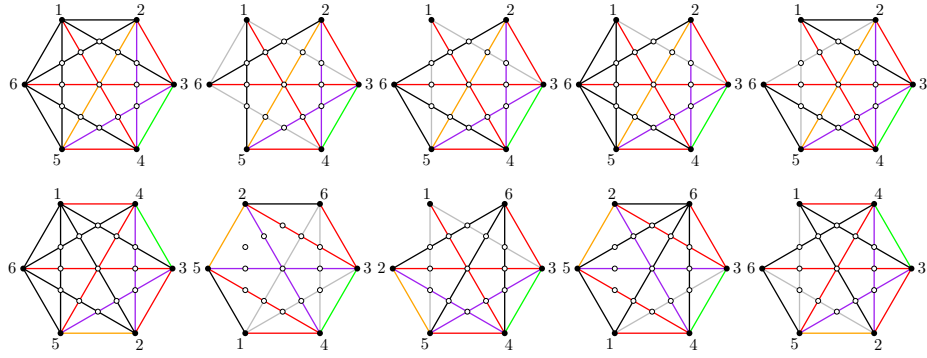


Fig. 7: The first row depicts sub-cases of the fourth case from Fig. 6 and the second row depicts for each of them an alternative permutation solving the problem.

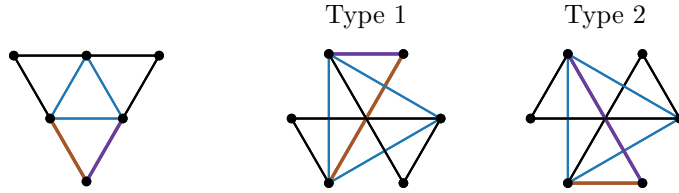


Fig. 8: An outerplanar graph G and its regular OORs.

SAT formulation described in Section 3. We call them Type 1 if the brown edge v_2v_4 passes through the center of the regular hexagon, and Type 2 if the purple edge v_1v_4 does, see Fig. 8. Let H be a supergraph of G such that the two vertices $u, w \in H - G$ are incident to v_2, v_4 and v_1, v_4 respectively; see Fig. 1c. None of the possibilities for adding u and w into the cyclic order of the vertices of G in Fig. 8 yields a regular OOR since in each case one of the non-edges incident to u or to w does not lie in the outer face; see Fig. 9 for permutations that satisfy the gap condition, but do not admit regular OORs. \square

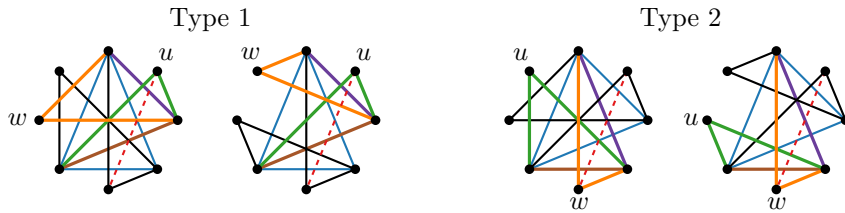


Fig. 9: All possibilities for adding u and w into the cyclic order of the vertices of G in Fig. 8. In each drawing, the red dashed non-edge misses the outer face.

B Omitted Proofs

Theorem 1 (\star). *Every 2-tree admits a reducible OOR with all vertices on the outer face.*

Proof. It follows readily from the definition of 2-trees that every 2-tree $T = (V, E)$ can be constructed through the following iterative procedure:

- (1) We start with one edge, called the *base* edge and mark its vertices as *inactive*. We stack any number of vertices onto the base edge and mark them as *active*. During the entire procedure, every present vertex is marked either as active or inactive. Moreover, once a vertex is inactive, it remains inactive for the remainder of the construction.
- (2) As an iterative step we pick one active vertex v and stack any number of vertices onto each of its two parent edges. All the new vertices are marked as active and v is now marked as inactive.
- (3) If there are active vertices remaining, repeat step (2).

Observe that step (2) is performed exactly once for each vertex that is not incident to the base edge. We construct a drawing of T by geometrically implementing the iterative procedure described above, so that after every step of the algorithm the present part of the graph is realized as a straight-line drawing satisfying the following set of invariants:

- (i) Each vertex v that is not incident to the base edge is associated with an open circular arc C_v that lies completely in the outer face and whose endpoints belong to the two parent edges of v . Moreover, v is located at the center of C_v and the parent edges of v are below v .
- (ii) Each non-edge intersects the circular arc of at least one of its incident vertices.
- (iii) For each active vertex v , the region R_v enclosed by C_v and the two parent edges of v is *empty*, meaning that R_v is not intersected by any edges, vertices, or circular arcs. (Combined with (i), it follows that R_v lies completely in the outer face.)
- (iv) Every vertex is incident to the outer face.

Once the procedure terminates, we have indeed obtained the desired drawing: invariants (i) and (ii) imply that each non-edge passes through the outer face and, hence, we have indeed obtained an OOR. Moreover, invariant (i) implies that each non-base edge is incident to the outer face of the drawing. The base edge will be drawn horizontally. By the second part of invariant (i), all vertices not incident to the base edge are above the base edge. Consequently, the base edge is incident to the outer face as well and, hence, the representation is reducible. Finally, by invariant (iv), every vertex belongs to the outer face.

Construction. To carry out step (1), we draw the base edge horizontally and place the stacked vertices on a common horizontal line above the base edge, see Fig. 2a. Circular arcs that satisfy the invariants are now easy to define.

Suppose we have obtained a drawing Γ of the graph obtained after step (1) and some number of iterations of step (2) such that Γ is equipped with a set of circular arcs satisfying the invariants (i)–(iv). We describe how to carry out another iteration of step (2) while maintaining the invariants.

Let v be an active vertex. By invariant (i), both parent edges of v are below v . Let e_ℓ and e_r be the left and right parent edge, respectively. Let $\ell_1, \ell_2, \dots, \ell_i$ and r_1, r_2, \dots, r_j be the vertices stacked onto e_ℓ and e_r , respectively. We refer to $\ell_1, \ell_2, \dots, \ell_i$ and r_1, r_2, \dots, r_j as the *new* vertices; the vertices of Γ are called *old*. We place all the new vertices on a common horizontal line h that intersects R_v above v , for an illustration see Fig. 2b. The vertices $\ell_1, \ell_2, \dots, \ell_i$ are placed inside R_v , to the right of the line $\overline{e_\ell}$ extending e_ℓ . Symmetrically, r_1, r_2, \dots, r_j are placed inside R_v , to the left of the line $\overline{e_r}$ extending e_r .

We place $\ell_1, \ell_2, \dots, \ell_i$ close enough to e_ℓ and r_1, r_2, \dots, r_j close enough to e_r such that the following properties are satisfied.

- a) None of the parent edges of the new vertices intersect C_v .
- b) For each new vertex, the unbounded open cone obtained by extending its parent edges to the bottom does not contain any vertices.

These properties are easy to achieve: let $\overline{e_\ell}(\alpha)$ be the line created by rotating $\overline{e_\ell}$ clockwise around v by angle α . Clearly, there is an angle α^* such that (A) the intersection $x(\alpha^*)$ of $\overline{e_\ell}(\alpha^*)$ with h lies in R_v and the line segment between $x(\alpha^*)$ and $e_\ell \setminus \{v\}$ does not intersect C_v , and (B) the open region that lies clockwise between $\overline{e_\ell}$ and $\overline{e_\ell}(\alpha^*)$ contains no vertices. We place the vertices $\ell_1, \ell_2, \dots, \ell_i$ to the left of $x(\alpha^*)$. Then property (A) guarantees property (a). Property (b) follows from property (B) and invariants (iii) and (iv) for Γ . The vertices r_1, r_2, \dots, r_j are placed symmetrically.

Correctness. It remains to show that the invariants are maintained.

Each of the old vertices retains its circular arc from Γ . By invariant (iii), the region R_v is completely contained in the outer face of Γ . Hence, it is easy to define circular arcs for the new vertices that satisfy invariant (i). To show that invariant (i) also holds for the circular arcs of the old vertices, we argue as follows: by the construction property (a), each parent edge e of a new vertex can be decomposed as follows: a line segment e_a that lies in R_v and a line segment e_b that lies in the triangle formed by the endpoints of the parent edges of v . By invariant (iii) for Γ , the region R_v is empty and, hence, e_a does not intersect the circular arc of any old vertex. By invariant (i) for Γ , the circular arcs of the old vertices lie in the outer face of Γ and, hence, it follows that e_b also does not intersect the circular arc of any old vertex. Consequently, invariant (i) is maintained for the circular arcs of old vertices.

Invariant (ii) is retained for the edges that join two old vertices since the circular arcs of these vertices have not been changed. Property (b) and the fact that all new vertices are placed on h imply that each of the non-edges incident

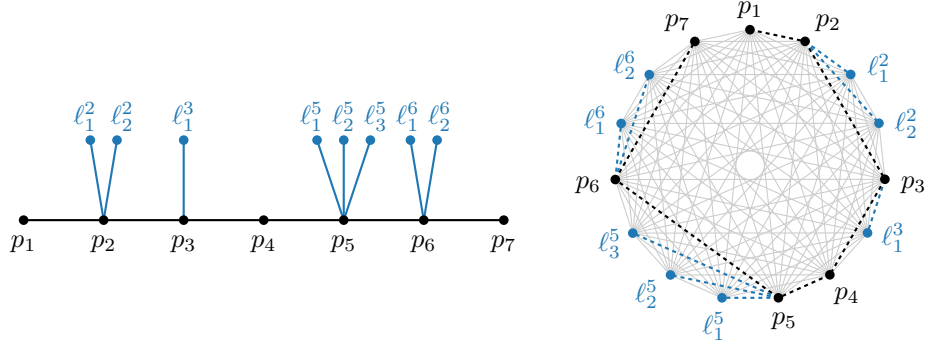


Fig. 10: A caterpillar and a regular OOR of its complement.

to a new vertex w intersect C_w . Hence, invariant (ii) is also satisfied for the new non-edges.

Invariant (iii) holds for the circular arcs of the new vertices by (iii) for v in Γ and by (i) for the new vertices. To see that invariant (iii) holds for the circular arcs of the old vertices, let $u \neq v$ be an old vertex. Let e be a parent edge of a new vertex and recall the definitions of e_a and e_b from above. The part e_a lies in R_v and e_b does not pass through the outer face of Γ . Hence, it follows that invariant (iii) is retained for u .

By invariant (iii) for Γ , the region R_v is contained in the outer face of Γ . Hence, by construction, invariant (iv) holds for v and the new vertices. Moreover, invariant (iv) is also retained for the remaining vertices since, by construction, the edges incident to new vertices intersect the outer face of Γ in R_v only. \square

Theorem 2 (\star). *For any tree T , the graph \bar{T} has a convex OOR if and only if T is a caterpillar.*

Proof. We prove the statement in two steps. First, we show that, for every caterpillar C , the graph \bar{C} has a circular OOR. Then we show that, for every tree T that is not a caterpillar, \bar{T} does not admit any convex OOR.

Let C be a caterpillar with central path $\langle p_1, p_2, \dots, p_r \rangle$. For $i \in \{2, \dots, r-1\}$, let $\ell_1^i, \ell_2^i, \dots, \ell_{n_i}^i$ be the leaves adjacent to path vertex p_i (if any). We arrange the vertices of \bar{C} in cyclic order as follows. First, we take the path vertices in the given order. Then, for each $i \in \{2, \dots, r-1\}$, we insert the leaves adjacent to vertex p_i between p_i and p_{i+1} into the cyclic order; see Fig. 10. The resulting order is $\langle p_1, p_2, \ell_1^2, \ell_2^2, \dots, \ell_{n_2}^2, \dots, p_{r-1}, \ell_1^{r-1}, \ell_2^{r-1}, \dots, \ell_{n_{r-1}}^{r-1}, p_r \rangle$.

Note that all non-neighbors of a vertex v of \bar{C} that succeed v in the circular order form an interval that starts right after v . Therefore, every non-edge of \bar{C} is incident to a path vertex p_i and intersects the outer face in the vicinity of p_i . Hence, the drawing of \bar{C} is a circular OOR. Since we fixed only the circular order of vertices and not their specific position, we can place them on a regular polygon.

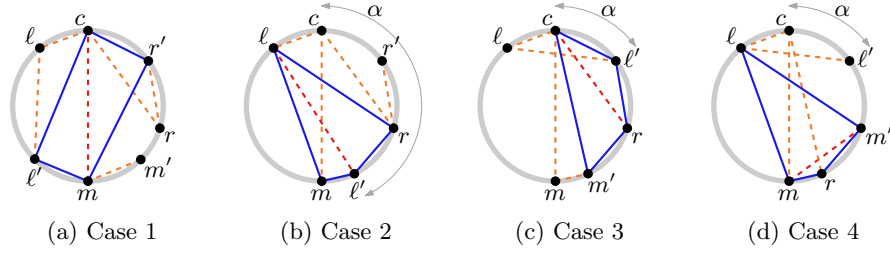


Fig. 11: Case distinction in the proof of [Theorem 2](#): (a) Case 1: cm is not intersected; (b) Case 2: ll' intersects cm , $\alpha \cap Y \neq \emptyset$; (c) Case 3: ll' intersects cm , $\alpha \cap Y = \emptyset$, and c, r, m' appear in this order in σ ; (d) Case 4: otherwise.

Now we prove the second part of the statement. Let Y be the tree that consists of a root c with three children ℓ, m and r , each of which has one child, namely ℓ', m' and r' , respectively; see [Fig. 12](#) (left). Let T be a tree that is not a caterpillar. Note that T has a subtree that is isomorphic to Y .

Let σ be any circular order of $V(Y)$. We now show that \bar{T} admits no convex OOR with respect to σ . To this end, we find an edge e of Y (that is, a non-edge of \bar{T}) that is a diagonal of a convex quadrilateral Q formed by four non-edges of Y . This yields our claim because any non-edge of Y must be an edge of \bar{T} (otherwise T would contain a cycle). Without loss of generality, let $\langle c, r, m, \ell \rangle$ be the order of c and its children in σ . We distinguish four cases.

Case 1: None of the edges of Y intersects cm ; see [Fig. 11a](#).

Then $e = cm$ lies inside the quadrilateral $Q = \square cr'm\ell'$ formed by non-edges of Y .

In the following three cases, we assume, without loss of generality, that ll' intersects cm . Let α be the open circular arc from c to ℓ' in clockwise direction.

Case 2: $\alpha \cap Y \neq \emptyset$, i.e., at least one vertex of Y lies in α , say r ; see [Fig. 11b](#).

Then $e = \ell\ell'$ lies inside the quadrilateral $Q = \square \ell r'\ell' m$.

In the remaining two cases, we assume that $\alpha \cap Y = \emptyset$.

Case 3: The vertices c, r , and m' appear in this order in σ ; see [Fig. 11c](#).

Then $e = cr$ lies inside the quadrilateral $Q = \square c\ell'rm'$.

Case 4: Otherwise; see [Fig. 11d](#).

Then $e = mm'$ lies inside the quadrilateral $Q = \square \ell m'rm$. □

[Figure 12](#) depicts the smallest tree that is not a caterpillar and hence does not have a convex OOR. It does, however, have an OOR.

Theorem 3 (\star). *Let $3 \leq k \leq n$. Then the graph $G_{n,k} = K_n - E(C_k)$, where C_k is a simple k -cycle, admits a convex OOR if and only if $k \in \{3, 4, n\}$.*

Proof. First, we show that, for $k \in \{3, 4, n\}$, the graph $G_{n,k}$ admits a convex OOR. To this end, we place the vertices v_1, \dots, v_k of C_k as an interval on a circle. If $k < n$, we place the remaining vertices in an arbitrary order, also as an

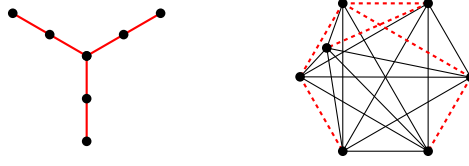


Fig. 12: The smallest tree Y that is not a caterpillar (left); a non-convex OOR of \bar{Y} .

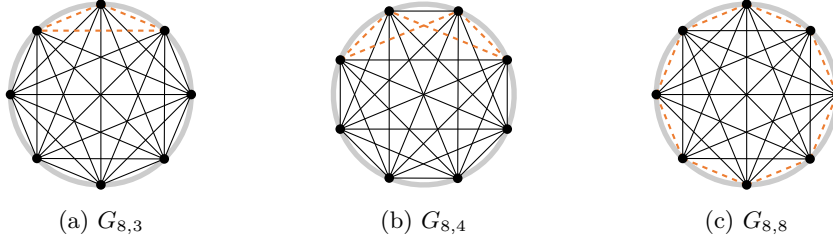


Fig. 13: Regular OORs of the graph $G_{n,k}$ for $n = 8$ and (a) $k = 3$, (b) $k = 4$, (c) $k = n$.

interval, on the same circle. For $k = 3$, the vertex order of C_3 is determined; see Fig. 13a. For $k = 4$, we place the vertices of C_4 in the order $\langle v_1, v_2, v_4, v_3 \rangle$; see Fig. 13b. For $k = n$, we take the vertex order of C_n ; see Fig. 13c. In the cases $k = 3$ and $k = n$, let $V' = V(G_{n,k})$. In the case $k = 4$, let $V' = V(G_{n,k}) \setminus \{v_2, v_4\}$ and note that v_2 and v_4 are adjacent in $G_{n,k}$. In all cases all vertices in V' satisfy the consecutive-neighbors property and V' covers all non-edges. Therefore, by Lemma 1, the graph $G_{n,k}$ admits a convex OOR with respect to the circular vertex order (depending on k) described above. Note that, in all cases, the OORs are even regular.

Now let $k \in \{5, \dots, n - 1\}$. The graph $G_{n,k}$ contains at least one vertex v that is adjacent to all other vertices. Let σ be any circular order of $V(G_{n,k})$ starting at v in clockwise direction. We prove that $G_{n,k}$ does not admit a convex OOR with respect to σ .

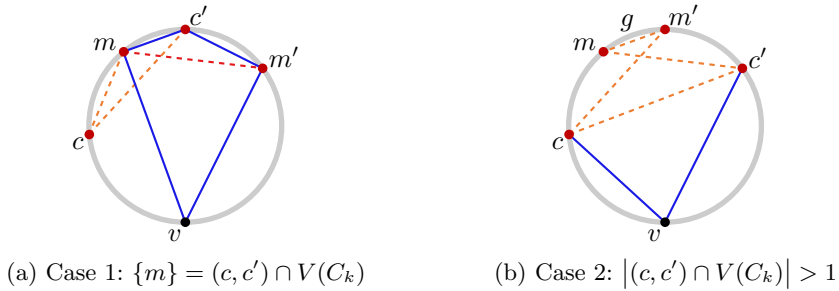


Fig. 14: Case distinction in the proof of Theorem 3.

To this end, let c be the first vertex of C_k after v in σ . Let c' be the last vertex in σ that is not adjacent to c . We consider two cases.

Case 1: There is only one vertex m of C_k in the interval (c, c') ; see Fig. 14a. Note that cm is a non-edge. Let m' be the other vertex that shares a non-edge with m . Note that m' lies between c' and v since c is the first vertex of C_k after v . Hence, mm' is a diagonal of the quadrilateral $Q = \square vmc'm'$. We argue that the edges of Q belong to $G_{n,k}$. For vm and vm' this is obvious, but it is also true for mc' and $c'm'$, otherwise the non-edges of $G_{n,k}$ would contain a C_3 or a C_4 , respectively. But $G_{n,k}$ has a simple k -cycle of non-edges with $k \geq 5$.

Case 2: There are at least two vertices of C_k in the interval (c, c') ; see Fig. 14b. Recall that cc' is a non-edge of $G_{n,k}$. For $G_{n,k}$ to admit a convex OOR with respect to σ , by Lemma 2, cc' would have to have a candidate gap g (that is, an edge of C_k). Due to the presence of the edges vc and vc' , the gap g must lie on the side of cc' that is opposite of v . Let m be the first endpoint of g , and let m' be the second endpoint (according to σ). Then, by the definition of a candidate gap, no edge connects the intervals $[c, m]$ and $[m', c']$. This implies that cm' and $m'c'$ are non-edges. Hence $\langle c, c', m, m' \rangle$ is a 4-cycle of non-edges – a contradiction to the fact that $G_{n,k}$ has a simple k -cycle of non-edges with $k \geq 5$.

In both cases, we have shown that $G_{n,k}$ does not admit a convex OOR with respect to σ . \square

Theorem 4 (\star). *The following graphs have reducible regular OORs:*
 1. every cactus; 2. every grid; 3. every outerpath.

Proof. **1.** For the given cactus, we first compute the block-cut tree (whose definition we recall below). Then, following the structure of the block-cut tree, we treat the blocks one by one. For each block, we insert its vertices as an interval into the vertex order of the subgraph that we have treated so far. Finally, we prove that the resulting circular vertex order yields a reducible regular OOR.

Recall that a *block-cut tree* of a biconnected graph is a tree that has a vertex for each *block* (i.e., a maximal 2-connected subgraph or bridge) and for each cut vertex. There is an edge in the block-cut tree for each pair of a block and a cut vertex that belongs to it; for an example of a block-cut tree of a cactus, see Fig. 15. We root the block-cut tree in an arbitrary block vertex and number the block vertices according to a breadth-first search traversal starting at the root.

In order to draw a cactus G , we treat its blocks one by one and insert the vertices of each block into the circular order, starting with the root block. For each further block B , there is a cut vertex v_B that belongs to a block that we have already inserted before. Hence, we insert the vertices of B as an interval between v_B and its clockwise successor in the circular order. For the root block B^* , let v_{B^*} be an arbitrary vertex of B^* .

Now we draw the current block B . If B is a single edge $v_B w$, we place w immediately behind v_B . If B is a cycle with k vertices ($k \geq 3$), we start with the cut vertex v_B and proceed in a zig-zag manner, mapping the vertices to positions

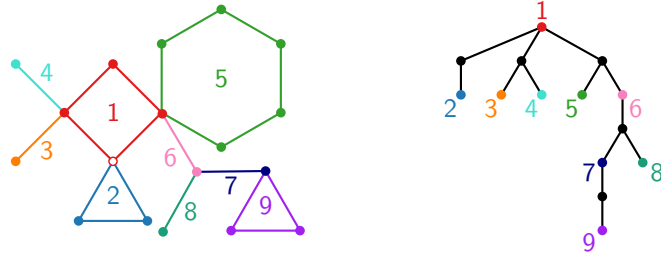


Fig. 15: A cactus and its block-cut tree. Black vertices correspond to cut vertices of the cactus.

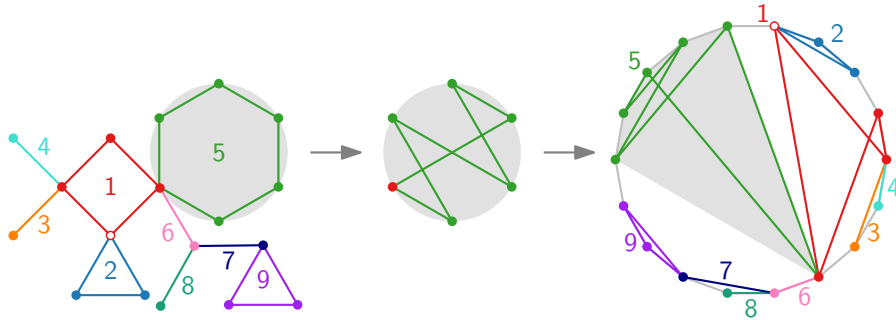


Fig. 16: Constructing a reducible regular OOR of a cactus.

1 (which is v_B), $k, 2, k - 1, \dots, \lceil (k + 1)/2 \rceil$; see Fig. 16. For $k \leq 4$ all vertices satisfy the consecutive-neighbors property. For $k \geq 5$, exactly two vertices do not satisfy this property, but these two vertices are adjacent, so by Lemma 1 all non-edges of B intersect the outer face as required.

Now we draw G by placing the vertices in the circular order on a circle that we just defined; the exact positions on the circle do not matter. Consider the convex hulls of the blocks in the drawing. Observe that any two of them share at most one vertex. Moreover, each convex hull lies completely in the outer face of the drawing. In the process described above, each block has its own OOR due to Lemma 1. Hence, the whole drawing is an OOR of G . The representation is reducible since each vertex has degree 2 within each block, and each block is surrounded by the outer face.

Since we do not specify the exact vertex positions on the circle, observe that (a) the representation can be chosen such that consecutive vertices are, for example, spaced equally (i.e., every set of n co-circular points is universal for the class of n -vertex cactus graphs) and (b) even cactus forests admit OORs.

2. For $i \geq 1$, let P_i be a path with i vertices v_1, v_2, \dots, v_i in this order and let G be the graph of a $k \times \ell$ square grid with $k, \ell \geq 2$. Formally, $G = P_k \square P_\ell$, where $G_1 \square G_2$ is the Cartesian product of graphs G_1 and G_2 . We place the vertices of

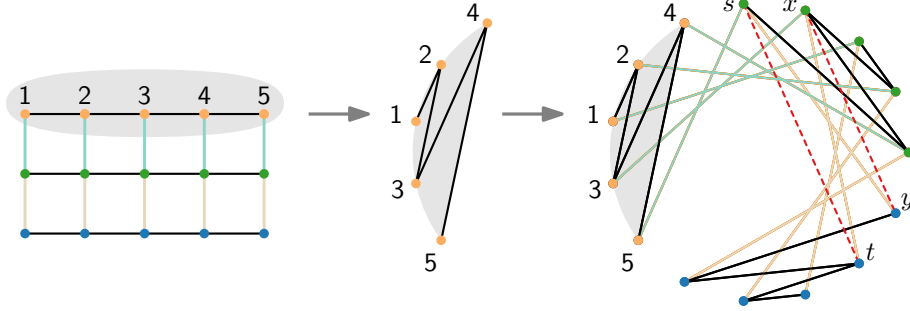


Fig. 17: Constructing a reducible regular OOR of the grid $P_5 \square P_3$.

each copy of P_k in the order $v_k, v_{k-2}, \dots, v_3, v_1, v_2, \dots, v_{k-1}$ if k is odd and in the order $v_k, v_{k-2}, \dots, v_2, v_1, v_3, \dots, v_{k-1}$ if k is even; see Fig. 17.

Within P_k , $v_{k-1}v_k$ is the longest edge; it has circular length $k - 1$ (that is, there are $k - 2$ other vertices between the endpoints of the edge on the circle). The copies of P_k are placed one after the other, which implies that every edge within a copy of P_ℓ (colored lightly in Fig. 17) has circular length exactly k .

We now show that every non-edge intersects the outer face. First, consider a non-edge $\{s, t\}$ that has circular length at least $k + 1$; see Fig. 17. Then it is longer than every edge of G ; hence it intersects the gap region between the first and last copy of P_k . Note that non-edges of length exactly k exist only between vertices of the first and the last copy of P_k , but these non-edges intersect the gap region between these two copies.

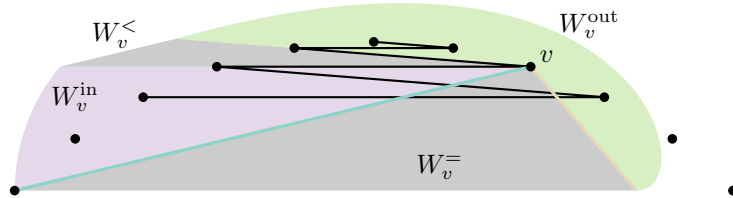


Fig. 18: The four wedges with respect to a vertex v of the grid graph $P_k \square P_\ell$. The black edges represent a copy of P_k . The two colored edges of length k belong to two different copies of P_ℓ .

Next, consider a non-edge $\{x, y\}$ that has length less than k . Every vertex v of G is incident to one or two edges of length k and one or two edges of length less than k . Let $W_v^=$ be the wedge with apex v formed by (and including) the length- k edge(s) – if there is just one such edge, then $W_v^=$ is the ray starting in v that contains this edge; see Fig. 18. Similarly, let $W_v^<$ be the wedge formed by (and including) the shorter edge(s). Hence the angular space around v is subdivided into four wedges; $W_v^=$, $W_v^<$, W_v^{in} , and W_v^{out} , where W_v^{out} is the (open) wedge

between $W_v^=$ and $W_v^<$ that, in the vicinity of v , contains the outer face of the drawing and W_v^{in} is the remainder of the plane. Note that $\{x, y\}$ is neither contained in $W_x^=$ nor in $W_x^<$. This is due to the fact that $W_x^=$ contains only vertices of distance greater than k and $W_x^<$ contains no vertices in its interior. For the same reasons, $\{x, y\}$ is neither contained in $W_y^=$ nor in $W_y^<$. It remains to show that $\{x, y\}$ lies in W_x^{out} or in W_y^{out} .

Suppose that $\{x, y\}$ lies in W_x^{in} and has circular length $j < k$. Then the edges in $W_x^<$ have length less than j . If y belongs to the same copy of P_k then, due to our layout of P_k , the edges in $W_y^<$ must be longer than j . (See for example the edge in Fig. 18 that starts in W_v^{in} .) This implies that $\{x, y\}$ lies in W_y^{out} .

It remains to consider the case that y lies in a different (but neighboring) copy of P_k , say, the next copy. Then, for $\{x, y\}$ to lie in W_x^{in} , x must lie in the “left” half (that is, $x \in \{v_k, v_{k-2}, \dots, v_1\}$) of its copy. Since $j < k$, y must lie in the left half of its copy, too. Due to our layout of P_k , the (short) edges in $W_y^<$ go to the other half of the copy. Therefore, the two long edges that define $W_y^=$ must lie between the short non-edge $\{x, y\}$ and the two short edges that define $W_y^<$. In other words, $\{x, y\}$ lies in W_y^{out} .

For reducibility, we can argue similarly as for the non-edges. Indeed, every edge of length k is adjacent to the gap region between the first and last copy of P_k . The shorter edges alternate in direction, so for $i \in \{1, \dots, k-1\}$, the edge $v_i v_{i+1}$ of P_k is adjacent to the outer face in the vicinity of vertex v_{i+1} .

3. Let G be an n -vertex outerpath, and let Γ be an outerpath drawing of G . We show that G admits a reducible regular OOR. The statement is trivial for $n \leq 3$, so assume otherwise. By reducibility and appropriately triangulating the internal faces of Γ , we may assume without loss of generality that each internal face of Γ is a triangle. Let the path $(t_1, t_2, \dots, t_{n-2})$ be the weak dual of Γ . Let V_i denote the set of vertices of G that are incident to the triangles t_1, t_2, \dots, t_i . By definition, V_1 contains a vertex v_1 of degree 2. For $4 \leq i \leq n$, let v_i denote the unique vertex in $V_{i-2} \setminus \bigcup_{j=1}^{i-3} V_j = \{v_1, v_2, \dots, v_{i-1}\}$; see Fig. 19(left). For $4 \leq i < n$, the vertex v_i is incident to an internal edge $e_i = v_i v_j$ of Γ such that $j < i$ and v_j belongs to the triangle t_{i-3} . Let $G_i = G[v_1, v_2, \dots, v_i]$. We iteratively construct reducible regular OORs $\Gamma_3, \Gamma_4, \dots, \Gamma_{n-2}$ of $G_3, G_4, \dots, G_{n-2}(= G)$, respectively. We create Γ_3 by arbitrarily drawing G_3 on the circle. To obtain Γ_i , for $4 \leq i < n$ from Γ_{i-1} , we consider the edge $e_i = v_i v_j$ and place v_i next to v_j on the circle, avoiding the (empty) arc of the circle that corresponds to e_{i-1} ; see Fig. 19(right). Vertex v_n is placed next to v_{n-1} , avoiding the arc that corresponds to e_{n-1} . (This yields that v_n has the consecutive neighbors property.)

For any three points a, b , and c on the circle C , let h_{ab}^{+c} be the open halfplane that is defined by the line ℓ_{ab} through a and b and that contains c . Similarly, let h_{ab}^{-c} be the open halfplane defined by ℓ_{ab} that does not contain c . Hence, $h_{ab}^{+c} \cup \ell_{ab} \cup h_{ab}^{-c} = \mathbb{R}^2$.

We keep the invariant that when we place w on C , h_{vw}^{-u} is empty and $h_{v'w}^{-u}$ contains only v (among the vertices placed so far).

Now we show that when we add the triangle $\triangle wv'v$, if a non-edge went through the outer face of the drawing Γ_{i-1} of G_{i-1} , it will continue to do so in

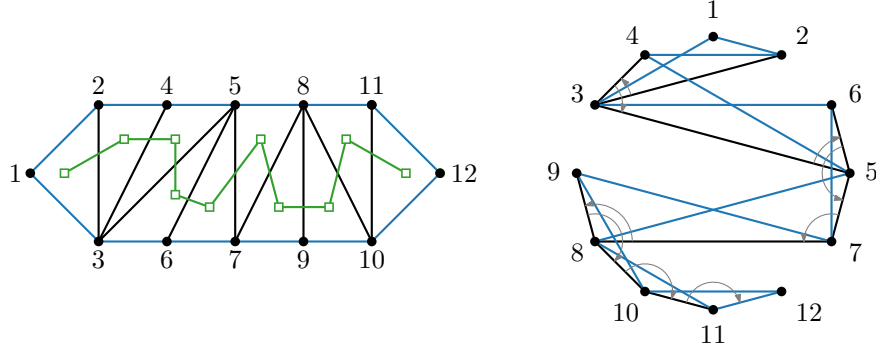


Fig. 19: A drawing Γ of an outerpath G and a reducible regular OOR of G based on Γ . Inner edges are black, outer edges are blue, weak dual edges are green.

the drawing Γ_i of G_i . We assume that $\triangle uv'v$ is oriented counterclockwise (as in Fig. 20). Let r be the rightmost neighbor of v in G_{i-1} (with respect to the

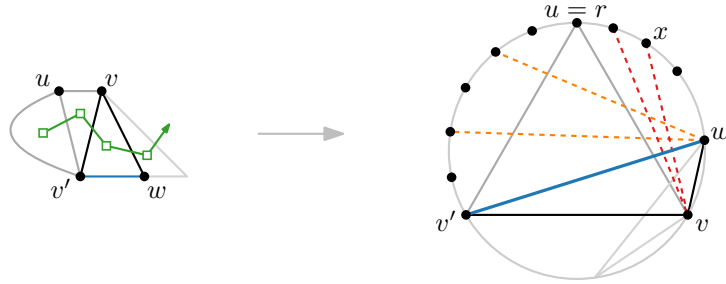


Fig. 20: Constructing a representation for outerpaths: the invariants are maintained.

ray from v to the center of C). Since u is a neighbor of v , $r = u$ (as in Fig. 20) or r lies strictly between u and v , but $r \neq w$ because $w \notin V(G_{i-1})$. Note that the halfplane $h_{v'w}^{-u}$ contains (the interior of) $\triangle wv'v$, but v is the only vertex in $h_{v'w}^{-u}$. Therefore, only non-edges incident to v can be affected by the addition of $\triangle wv'v$, and among these only the ones that go through the outer face of Γ_{i-1} in the vicinity of v . These are the non-edges (dashed red in Fig. 20) that are incident to v and lie in the halfplane h_{rv}^{-u} that is induced by rv and does not contain v' . Any such non-edge $\{v, x\}$ intersects $v'w$ since v and x lie on different sides of $v'w$. The intersection point of $\{v, x\}$ and $v'w$ lies on the outer face of Γ_i because $h_{v'w}^{-u}$ contains only v and, in G_i , w is incident to only v and v' . This proves our claim regarding the “old” non-edges.

The “new” non-edges (orange dashed in Fig. 20) are all incident to w and lie in $h_{v'w}^{-v}$. Since the two neighbors of w , namely v and v' , are consecutive in Γ_i , all non-edges incident to w go through the outer face.

It remains to show that T_i is reducible. For the two new edges incident to w it is clear that they are both part of the outer face – at least in the vicinity of w . Since h_{vw}^- is empty, the only old edge that is affected by the addition of $\Delta wv'v$ is the edge vr . It used to be part of the outer face at least in the vicinity of v . Arguing similarly as we did above for the non-edge $\{v, x\}$, we claim that the intersection point of vr and $v'w$ lies on the outer face. \square

A graph is *convex round* if its vertices can be circularly enumerated such that the open neighborhood of every vertex is an interval in the enumeration. A *bipartite graph* with bipartition (U, W) of the vertex set is *convex* if U can be enumerated such that, for each vertex in W , its neighborhood is an interval in the enumeration of U . By definition, every convex round and convex bipartite graph admits a circular order such that every vertex satisfies the consecutive-neighbors property. This yields the following.

Observation 2. *Every convex round and convex bipartite graph admits a regular OOR.*